Vol. **110** (2006) *ACTA PHYSICA POLONICA A* No. 6

Dielectric and X-ray Studies of Eleventh and Twelfth Members of Two Isothiocyanato Mesogenic Compounds

M. Jasiurkowska[a], A. Budziak[a], J. Czub[b] and S. Urban[b,*]

[a]H. Niewodniczański Institute of Nuclear Physics, Polish Academy of Sciences
Radzikowskiego 152, 31-342 Kraków, Poland
[b]Institute of Physics, Jagiellonian University
Reymonta 4, 30-059 Kraków, Poland

(Received September 11, 2006; in final form November 27, 2006)

Results of the dielectric and X-ray studies of the long-alkyl-chain members (n = 11, 12) of two homologous series: nBT (4-n-alkyl--4′-isothiocyanato-biphenyl) and nCHBT (4-*trans*-4′-n-alkyl-cyclohexyl--isothiocyanato-benzene) in their liquid crystalline phases are presented. These compounds exhibit different polymorphisms: the nematic phase for nCHBTs and the smectic E and smectic A phases for nBTs. The dielectric measurements were performed in a wide frequency range of 1 kHz–3 GHz. The layer thickness in the smectic E and smectic A phases and the orthorhombic unit cell parameters of the smectic E phase were determined using the small angle X-ray diffraction method. In the smectic E phase the layer-thickness-to-molecular-length ratios are found to be close to 1. The corresponding ratios observed for the smectic A phase of nBTs are considerably higher ($\approx$ 1.24), which indicates that an alternating head-to-tail arrangement of molecules in the layers is favored. The rotational dynamics of molecules in the smectic E phases is discussed in relation to their packing in a unit cell.

PACS numbers: 61.10.Eq, 61.66.Hq, 64.70.Md, 77.22.–d, 77.22.Gm

1. Introduction

Generally, the anisotropy of molecular shape is the necessary condition for creation of the liquid crystalline (LC) state. However, the problem which of the

*corresponding author; e-mail: ufurban@cyf-kr.edu.pl

molecular parameters act in favor of the appearance of a given phase or sequence of phases belongs to the most intriguing questions in this field. Therefore the studies of the substances having, on the one hand, a simple chemical structure and, on the other hand, exhibiting quite different phase sequences, seem to be useful. For example, two well-known alkyl-biphenyl homologous series, nCBs and nBTs, differ by the terminal polar group only (–CN and –NCS, respectively) but they display considerably different phase behavior under atmospheric as well as elevated pressures [1]. In the present work we have chosen the eleventh and twelfth members of two homologous series that differ by one ring in the molecular cores: 4-*trans*-4′-*n*-alkyl-cyclohexyl-isothiocyanato-benzene (nCHBT) and 4-*trans*-4′-*n*--alkyl-isothiocyanato-biphenyl (nBT).

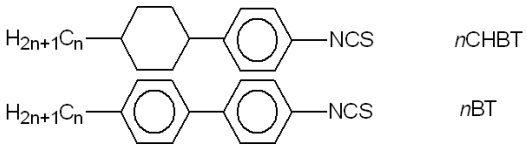

However, they exhibit quite different phase diagrams [2]:

$$\mathrm{Cr} \overset{48.1^\circ\mathrm{C}}{\longrightarrow} \mathrm{N} \overset{53.6^\circ\mathrm{C}}{\longrightarrow} \mathrm{Is} \quad \text{11CHBT},$$

$$\mathrm{Cr} \overset{51.0^\circ\mathrm{C}}{\longrightarrow} \mathrm{N} \overset{52.4^\circ\mathrm{C}}{\longrightarrow} \mathrm{Is} \quad \text{12CHBT},$$

and [1]

$$\mathrm{Cr} \overset{54.6^\circ\mathrm{C}}{\longrightarrow} \mathrm{SmE} \overset{59.9^\circ\mathrm{C}}{\longrightarrow} \mathrm{SmA} \overset{62.5^\circ\mathrm{C}}{\longrightarrow} \mathrm{Is} \quad \text{11BT},$$

$$\mathrm{Cr} \overset{53.8^\circ\mathrm{C}}{\longrightarrow} \mathrm{SmE} \overset{55.6^\circ\mathrm{C}}{\longrightarrow} \mathrm{SmA} \overset{60.6^\circ\mathrm{C}}{\longrightarrow} \mathrm{Is} \quad \text{12BT},$$

where Cr — crystalline, SmE ($\mathrm{S_E}$) — smectic E, SmA ($\mathrm{S_A}$) — smectic A, N — nematic, and Is — isotropic phase. The dielectric properties of the examined substances (static and dynamic) together with the X-ray data yielding information about molecular arrangements and packing in the LC phases will be discussed.

2. Experimental

All substances were synthesized in the Institute of Chemistry, the Military University of Technology, Warsaw.

The dielectric relaxation spectra, $\varepsilon^*(f) = \varepsilon'(f) - \mathrm{i}\varepsilon''(f)$, were recorded using an impedance analyzer HP 4192A in the frequency range of 1 kHz–30 MHz. The samples in the N phase were oriented by a magnetic field of 0.8 T. Two experimental geometries were applied: $\boldsymbol{E} \parallel \boldsymbol{B}$ and $\boldsymbol{E} \perp \boldsymbol{B}$, enabling the measurement of the $\varepsilon_\parallel$ and $\varepsilon_\perp$ permittivity tensor components, respectively. The thickness of the samples was 0.7 mm. The temperature was stabilized within ± 0.1 K. In the isotropic phase a time domain spectrometer (TDS) was employed that covers the frequency range of 10 MHz–3 GHz [3]. All measurements were carried out while

cooling the samples. The supercooling of the LC phases, sometimes by more than 10°C, was observed.

X-ray studies were performed on an X'Pert PRO (PANalytical) diffractometer using the Cu K_α radiation (λ = 1.54178 Å) and a graphite monochromator. Samples were placed in a nickel-plated copper sample holder of dimensions $18 \times 9 \times 0.2$ mm^3. The temperature of a sample was stabilized (accuracy ±0.1°C) with the continuous flow cryostat supplied by an Anton Paar Co. The samples in the smectic A phase were not oriented. Prior to the measurements of the smectic E phase the samples were melted, cooled to room temperature with the rate of 10 deg/min, and finally crushed. After each cooling stage the samples were allowed to equilibrate for about 5 min.

3. Results

3.1. Dielectric studies

The static permittivity values obtained for the isotropic and LC phases of 11CHBT, 12CHBT, 11BT, and 12BT are shown in Fig. 1. The smectic phases of 11BT and 12BT could not be oriented. In the isotropic phase the values of the static permittivity measured for both series of compounds are comparable and display the usual decrease with the elongation of the alkyl chain (cf. Table I). The dielectric anisotropy as a function of temperature, $\Delta\varepsilon = \varepsilon_\parallel - \varepsilon_\perp$, in the nematic phase of 11CHBT and 12CHBT is presented in Fig. 2a. The values obtained in this paper are larger than those reported in [2], probably due to a better alignment of the samples.

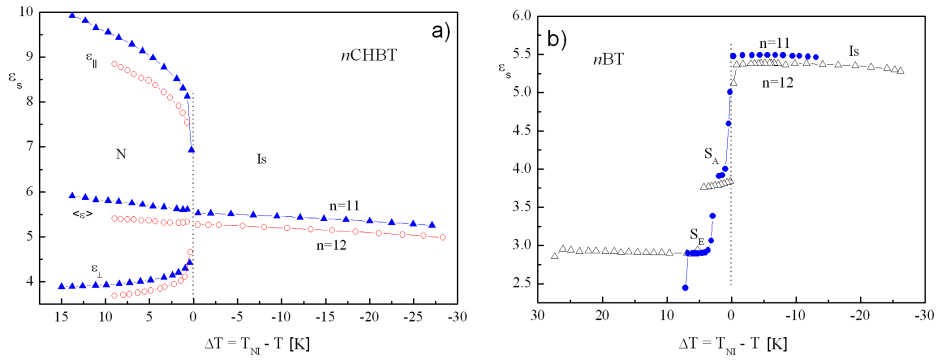

Fig. 1. Static permittivity vs. temperature reduced to the clearing points in the isotropic phase (Is) and mesophases (N, S_A, S_E) of 11CHBT and 12CHBT (a) and 11BT and 12BT (b).

The results of dielectric relaxation measurements in the isotropic phase of 11CHBT and 11BT are presented in Fig. 3 in the form of the Cole–Cole plots. They reveal two modes that can be attributed to the molecular rotations around the

TABLE I

The parameters determined from the dielectric measurements of 11CHBT, 12CHBT, 11BT, and 12BT (the meaning of symbols — see the text).

Substance	11CHBT	12CHBT	11BT	12BT
$\varepsilon_{\mathrm{Is}}$	5.52	5.28	5.05	4.94
β [°]	21.8	21.8	23.0	22.8
$\Delta\varepsilon$ ($\Delta T = 9$ K)	5.54	5.16	–	–
$g = \tau_{\mathrm{N,A}}/\tau_{\mathrm{Is}}$	3.7	4.3	3.7	4.1
$g = \tau_{\mathrm{E}}/\tau_{\mathrm{A}}$	–	–	19.7	12.4
ΔH_{Is}(l.f.) [kJ/mol]	29.4	26.7	32.2	27.9
ΔH_{Is}(h.f.) [kJ/mol]	20	21.7	29.3	23.5
ΔH_{N}(l.f.) [kJ/mol]	93.6	99.2	–	–
ΔH_{A}(l.f.) [kJ/mol]	–	–	–	55.5
ΔH_{E}(l.f.) [kJ/mol]	–	–	80.5	80.5

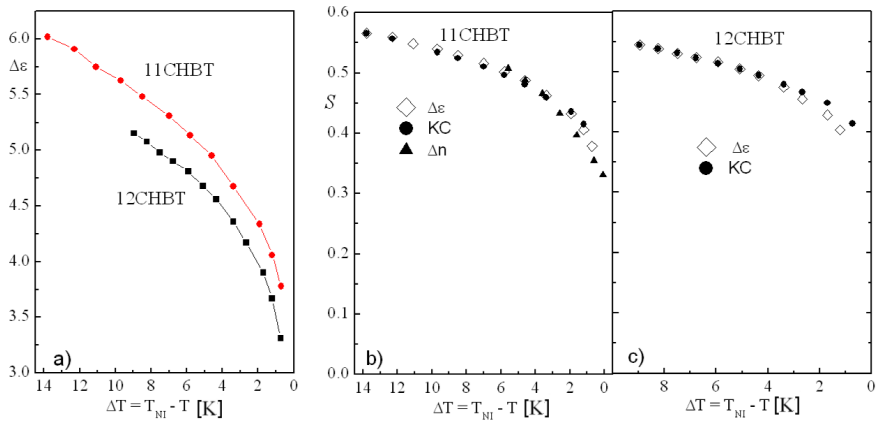

Fig. 2. The dielectric anisotropy $\Delta\varepsilon = \varepsilon_{\parallel} - \varepsilon_{\perp}$ (a) and the order parameter S (b, c) calculated according to the Maier–Meier equation (2) — $\Delta\varepsilon$, Coffey et al. approach (KC) [13, 14], and from the optical anisotropy — Δn [2], versus the relative temperature ΔT in the nematic phase of 11CHBT and 12CHBT.

principal inertia axes. The data were analyzed using a superposition of two Debye-type formulae,

$$\varepsilon^*(\omega) - \varepsilon_\infty = \frac{\delta\varepsilon_{\mathrm{l.f.}}}{1+\mathrm{i}\omega\tau_{\mathrm{l.f.}}} + \frac{\delta\varepsilon_{\mathrm{h.f.}}}{1+\mathrm{i}\omega\tau_{\mathrm{h.f.}}}, \tag{1}$$

where $\delta\varepsilon_{\mathrm{l.f.}}$ and $\delta\varepsilon_{\mathrm{h.f.}}$ are the dielectric increments ($\delta\varepsilon = \varepsilon_{\mathrm{s}} - \varepsilon_\infty$, where ε_{s} are the static and ε_∞ high frequency permittivities, respectively), $\tau_{\mathrm{l.f.}}$ and $\tau_{\mathrm{h.f.}}$ are

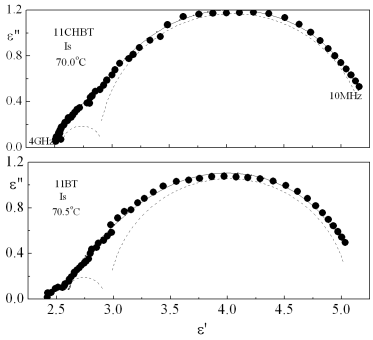

Fig. 3. TDS spectra in the form of the Cole–Cole plots for 11CHBT and 11BT in the isotropic phase. The dashed lines display the contributions from the high frequency and low frequency relaxation modes, cf. Eq. (1).

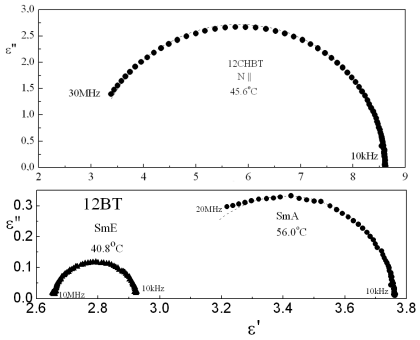

Fig. 4. Cole–Cole plots for the 12CHBT and 12BT in the LC phases.

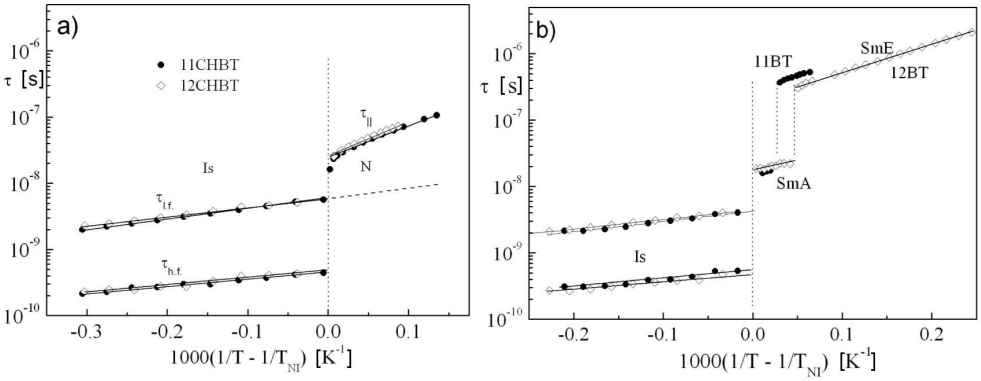

Fig. 5. Arrhenius plots (in the reduced scale) for four substances studied in different phases: (a) nCHBTs, (b) nBTs.

the relaxation times for the low and high frequency relaxation processes, respectively. The high frequency process can be visible due to an inclination of the

long molecular axis from the *para*-axis of the benzene ring. It is a common feature of this type of compounds (see, for example, [4–6]). According to the well-known Onsager equation we have $A_{\mathrm{h.f.}}/A_{\mathrm{l.f.}} \sim (\mu_{\mathrm{t}}/\mu_{\mathrm{l}})^2 = \tan^2\beta$, where $A = [(\varepsilon_{\mathrm{s}} - \varepsilon_\infty)(2\varepsilon_{\mathrm{s}} + \varepsilon_\infty)]/[\varepsilon_{\mathrm{s}}(\varepsilon_\infty + 2)^2]$ for a given relaxation mode, where β is the angle between the dipole moment and the long axis corresponding to the lowest moment of inertia. The estimated β-values are listed in Table I. The low frequency processes observed in the LC phases are well described by a single Debye formula (Fig. 4).

The relaxation times calculated for particular substances in different phases are presented in Fig. 5 in the form of the Arrhenius plots reduced to the clearing points. The activation enthalpy values calculated from the slopes of the lines fitted to the data are listed in Table I.

3.2. X-ray studies

In the SmA phase of 11BT and 12BT one strong (001) and one weak (002) reflections were detected corresponding to the layer and bilayer thicknesses, respectively, cf. Fig. 6a. In Fig. 6b diffraction patterns for the SmE phase of 11BT and 12BT are shown. From six to eight Bragg reflections observed at different temperatures were indexed assuming an orthorhombic unit cell [7]. The experimental and calculated X-ray parameters for one temperature in the E phase are listed in Table II. Figure 7a shows the temperature dependence of the layer thickness d

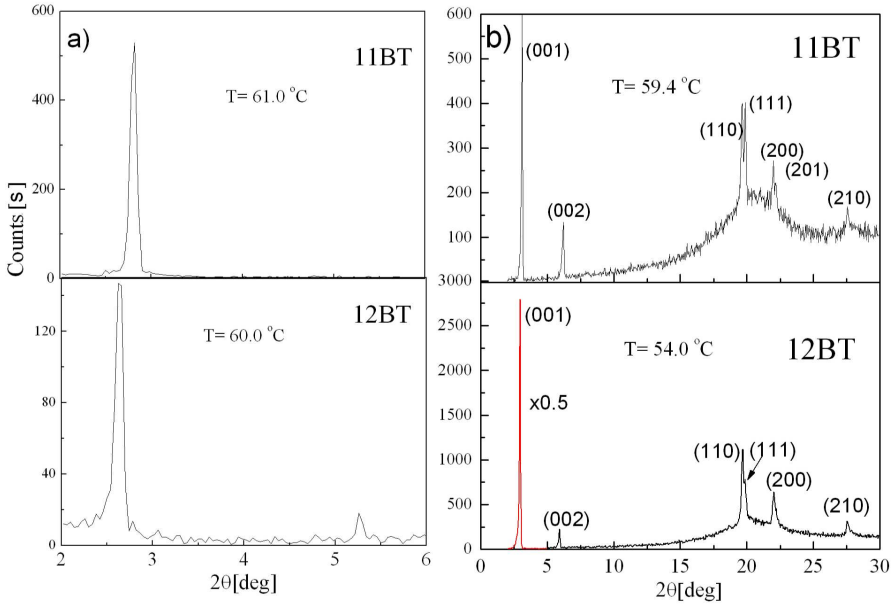

Fig. 6. Diffraction patterns recorded in the SmA (a) and SmE (b) phases of 11BT and 12BT.

TABLE II

The X-ray data in the SmE phase of 11BT and 12BT.

Compound	Intensity [counts/s]	d_{exp} [Å]	d_{cal} [Å]	Miller indices	Lattice constants [Å]	$V_{u.c.}$ [Å^3]
	312	28.43	28.43	(001)	$a = 8.07 \pm 0.02$	1254
	66	14.21	14.22	(002)	$b = 5.45 \pm 0.02$	
11BT	202	4.52	4.50	(110)	$c = 28.43 \pm 0.05$	
	198	4.45	4.46	(111)		
59.4°C	135	4.04	4.04	(200)		
	110	4.01	4.00	(201)		
	83	3.23	3.24	(210)		
	2715	29.76	29.76	(001)	$a = 8.07 \pm 0.02$	1313
	140	14.91	14.88	(002)	$b = 5.47 \pm 0.02$	
12BT	534	4.52	4.52	(110)	$c = 29.76 \pm 0.05$	
	369	4.47	4.46	(111)		
54.0°C	320	4.03	4.03	(200)		
	252	4.01	3.99	(201)		
	136	3.23	3.24	(210)		

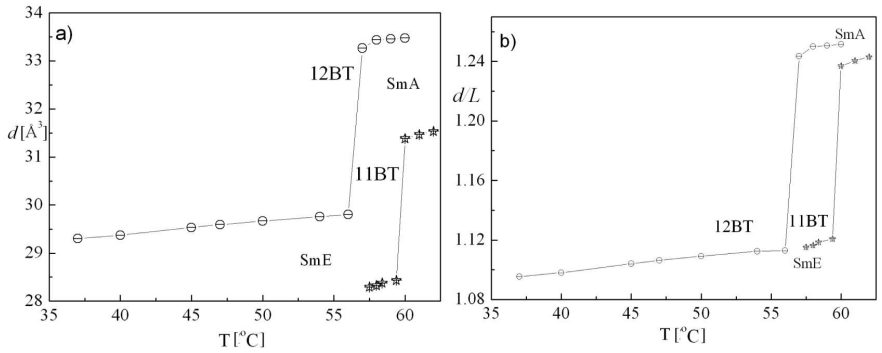

Fig. 7. The layer spacing d (a) and the ratio d/L (b) vs. temperature in the smectic phases of 11BT and 12BT.

for both compounds studied, whereas in Fig. 7b the layer-thickness-to-molecular-length ratios d/L as a function of temperature are depicted. The molecular lengths L were calculated using the Hyper Chem 7.5 program. The values obtained for the most extended conformations are $L = 23.62$ Å for 11BT and 25.37 Å for 12BT. The volumes of the unit cells calculated for 11BT and 12BT are presented in Fig. 8 as a function of temperature. The volumetric thermal-expansion coefficient calculated for 12BT amounts to $\alpha = 1.09 \times 10^{-3}$ K^{-1} and is larger than the value of 0.84×10^{-3} K^{-1} obtained for 8BT from the pVT measurements [8].

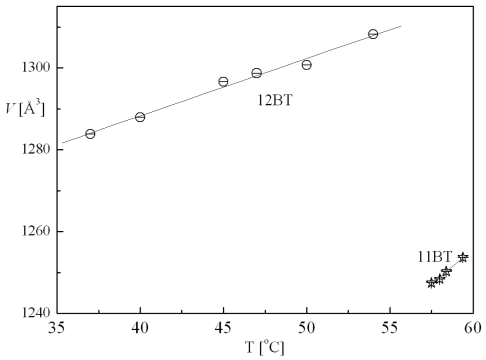

Fig. 8. The temperature dependence of the unit cell volume in the smectic E phase of 11BT and 12BT.

4. Discussion

The dielectric properties of an LC phase are determined by the number of polar groups and their positions in the molecule. Substances studied in the present work have only one polar group, i.e. –NCS with the dipole moment of $\mu =$ 3.5 D along the *para*-axis of the benzene ring [9]. However, due to conformational motions of the alkyl tail, the axis corresponding to the lowest moment-of-inertia value (the long molecular axis) is inclined from the *para*-axis by *ca.* 22° in both homologous series (see Table I). For this reason both rotations around the short and long molecular axes are visible in the relaxation spectra of the isotropic phase (Fig. 3). It can be seen (cf. Table I) that the replacement of the benzene ring by the cyclohexyl one increases the static permittivity values in the isotropic phase. Unfortunately, the lack of the density data for nBTs does not allow us a detailed discussion of this effect.

We have shown recently [10, 11] that for substances with large positive dielectric anisotropy the Maier and Meier equation [12], as well as the approach by Coffey et al. [13, 14] based on the retardation factor, can give valuable information on the order parameter $S(T) = \langle P_2(\cos^2\theta)\rangle$ as a function of temperature and pressure (θ is the angle between the long molecular axis and the director $\boldsymbol{n}$). The above-mentioned procedures were applied to the present substances.

According to the Maier and Meier theory [12] the dielectric anisotropy is given by

$$\Delta\varepsilon = \varepsilon_{\parallel} - \varepsilon_{\perp} = \varepsilon_0^{-1} N_0 h F \left[\Delta\alpha - F\frac{\mu}{2k_{\mathrm{B}}T}(1 - 3\cos^2\beta)\right] S, \tag{2}$$

where ε_0 is the permittivity of free space, N_0 — the number density, h and F — the local field factors dependent upon the mean dielectric permittivity, β — the angle between the dipole moment $\boldsymbol{\mu}$ and the long molecular axis, $\Delta\alpha$ — the anisotropy of the molecular polarizability. For strongly polar compounds $\Delta\alpha$ can be ignored in (2) and the following simplified relation between $\Delta\varepsilon$ and S holds

$$S(T) \sim T\Delta\varepsilon(T)/hF^2. \tag{3}$$

Additionally, the Haller formula [15] was assumed, i.e.,

$$S(T) = S_0(\Delta T)^\gamma, \tag{4}$$

where $S_0 = 1/T_{\rm NI}^\gamma$ and $\Delta T = T_{\rm NI} - T$ is the reduced temperature. The order parameter values calculated using Eqs. (3) and (4) are shown in Fig. 2b.

Coffey et al. [13, 14] related the order parameter to the nematic potential σ:

$$\sigma \approx \frac{3S(5-\pi S)}{2(1-S^2)}. \tag{5}$$

The potential σ can be obtained from the retardation factor $g_\parallel = \tau_\parallel/\tau_0$ data (τ_0 corresponds to the longitudinal relaxation time extrapolated from the isotropic liquid to the nematic phase — cf. the dashed line in Fig. 5a). The S-values obtained in this way are also presented in Fig. 2b,c. Additionally, the S-data obtained from the refractive index measurements [2] are shown in Fig. 2b. The agreement between these sets of data is very good.

In the isotropic phase of the compounds under study the parameters characterizing the molecular dynamics are very similar (compare Fig. 5 and Table I). The transition to the LC phases is accompanied by various dynamical effects. The longitudinal relaxation time is retarded by the factor $g \approx 4$ in the case of the Is–N and Is–SmA transitions, whereas for the SmA–SmE transition the retardation factor exceeds 12. The values of the activation barrier hindering the flip-flop molecular motions strongly depend on the phase (Table I): the largest values are for the N phase of nCHBTs ($\approx$ 100 kJ/mol), the smallest are for the Is phase ($\approx$ 30 kJ/mol). Surprisingly, in the A phase of 12BT $\Delta H_\parallel$ equals 55 kJ/mol only (for 11BT it was not calculated due to a narrow range of the A phase). The effect of lowering of the activation barrier in the A phase has been discussed in [16] for the higher members of the alkyl-cyanobiphenyl homologous series. The activation barriers in the E phase of 11BT and 12BT ($\approx$ 80 kJ/mol) are slightly larger than these obtained for shorter members of this homologous series [17]. The dynamical properties of molecules in the E phase will be discussed below taking into account the X-ray data.

The X-ray data enable us to relate the molecular lengths corresponding to *all-trans* conformation of the alkyl tail to the thicknesses of smectic layers. Figure 7b shows that the ratio d/L is slightly greater than 1 for the E phase, whereas its value exceeds 1.24 in the A phase. This observation is at variance with the claim that the isothiocyanato compounds should not form antiparallel dipole–dipole correlations in the LC phases (see, e.g., [18, 19]).

For the SmE phase of 11BT and 12BT the unit cell parameters were determined and the unit cell volumes were calculated. The results are shown in Fig. 8. Let us note that the a and b lattice constants are practically temperature independent and the volume changes are driven by the temperature behavior of the c parameter (the layer thicknesses). For both compounds the c-values are com-

parable with the molecular lengths obtained for the most extended conformations of terminal groups. The values of the b lattice constant are typical of compounds with aromatic cores [16, 20] and should correspond to the molecular diameters. If so, the lattice constant a characterizes the distance between the centers of mass of molecules in the cell. The ratio $a/L \approx 0.33$ gives the scale of a fluctuation in molecular positions which will make a sufficient space for a molecule to perform a flip-flop rotational jump. It is facilitated by a loose packing of molecules in the cells. Assuming $Z = 2$ molecules per cell, one can calculate the packing parameter $p = ZV_{\mathrm{m}}/V_{\mathrm{u.c}}$, where the volumes of molecules V_{m} have been calculated using the Cerius 2 program assuming the *all-trans* configuration (V_{m} equals 365.8 Å^3 for 11BT and 378.6 Å^3 for 12BT, the volumes of the unit cell $V_{\mathrm{u.c.}}$ are listed in Table II). Within the E phase the obtained p parameters vary from 0.584 to 0.568 for 11BT and from 0.577 to 0.590 for 12BT with rising temperature. These values are typical of the plastic crystalline (ODIC) phases [21, 22], and are smaller than those calculated for other compounds in the E phase [16, 23] ($p \approx 0.63$–0.67) having, however, shorter alkyl chains.

5. Conclusions

The substances belonging to two homologous series which differ in one ring in the molecular cores show different polymorphisms (N for nCHBTs and SmE for nBTs). Dielectric studies of the isotropic phase indicate close similarity of the molecular dynamics in both types of examined compounds. Conformational motions of the long alkyl chains and/or flexibility of the cyclohexyl ring result in an inclination of the long molecular axes from the *para*-axis of the benzene ring and facilitate the flip-flop rotation jumps in the LC phases. Common studies of the molecular motions such as the end-over-end rotations together with their packing in the (soft-crystalline) SmE phase allow us to better understand the relationship between both these factors. The molecules in the SmE phase are arranged in the orthorhombic structure but they form a rather loosely packed system — only *ca.* 60% of the unit cells are occupied by the molecular bodies. It facilitates the long-range fluctuations of the molecular centers of mass which creates a space necessary for the voluminous flip-flop jumps of molecules. A large number of the "lattice" defects, typical of the ODIC phases [21, 22], is a favorable factor in creation of the space.

Acknowledgments

Financial support from the Polish Ministry of Sciences grant no. 1 PO3B 060 28 is gratefully acknowledged.

References

[1] S. Urban, J. Czub, R. Dąbrowski, A. Würflinger, *Phase Trans.* **79**, 331 (2006).

[2] P. Sarkar, P. Mandal, S. Paul, R. Paul, R. Dąbrowski, K. Czupryński, *Liq. Cryst.* **30**, 507 (2003).

[3] B. Gestblom, in: *Relaxation Phenomena*, Eds. W. Haase, S. Wróbel, Springer--Verlag, Berlin 2003, Ch. 1.2.

[4] S. Urban, B. Gestblom, A. Würflinger, *Mol. Cryst. Liq. Cryst.* **331**, 113 (1999).

[5] J. Jadżyn, G. Czechowski, R. Douali, C. Legrand, *Liq. Cryst.* **26**, 1591 (1999).

[6] J. Jadżyn, L. Hellemans, G. Czechowski, C. Legrand, R. Douali, *Liq. Cryst.* **27**, 613 (2000).

[7] S. Diele, *Phys. Status Solidi A* **25**, K183 (1974).

[8] A. Würflinger, S. Urban, *Liq. Cryst.* **29**, 799 (2002).

[9] P. Kędziora, J. Jadżyn, *Acta Phys. Pol. A* **77**, 605 (1990).

[10] S. Urban, B. Gestblom, W. Kuczyński, S. Pawlus, A. Würflinger, *Phys. Chem. Chem. Phys.* **5**, 924 (2003).

[11] S. Urban, B. Gestblom, S. Pawlus, *Z. Naturforsch. A* **58**, 357 (2003).

[12] W. Maier, G. Meier, *Z. Naturforsch. A* **16**, 262, 470 (1961).

[13] W.T. Coffey, Yu.P. Kalmykov, J.P. Waldron, *Liq. Cryst.* **18**, 677 (1995).

[14] Yu.P. Kalmykov, W.T. Coffey, *Liq. Cryst.* **25**, 329 (1998).

[15] I. Haller, *Prog. Solid State Chem.* **10**, 103 (1975).

[16] S. Urban, J. Przedmojski, J. Czub, *Liq. Cryst.* **32**, 619 (2005).

[17] S. Urban, K. Czupryński, R. Dąbrowski, B. Gestblom, J. Janik, H. Kresse, H. Schmalfuss, *Liq. Cryst.* **28**, 691 (2001).

[18] K. Czupryński, R. Dąbrowski, J. Baran, A. Żywociński, J. Przedmojski, *J. Phys. (France)* **47**, 1577 (1986).

[19] R. Dąbrowski, J. Przedmojski, J. Baran, B. Pura, *Cryst. Res. Technol.* **21**, 567 (1986).

[20] S. Diele, D. Jaeckel, D. Demus, H. Sackmann, *Cryst. Res. Technol.* **17**, 1591 (1982).

[21] S. Urban, *Adv. Mol. Relax. Inter. Processes* **21**, 221 (1981).

[22] P. Nagrier, L.C. Pardo, J. Salud, J.L. Tamarit, M. Barrio, D.O. Lopez, A. Würflinger, D. Mondieig, *Chem. Mater.* **14**, 1921 (2002).

[23] S. Urban, J. Czub, R. Dąbrowski, H. Kresse, *Liq. Cryst.* **32**, 119 (2005).